agronomy

MDPI

Article

Accuracy of Estimated Crop Evapotranspiration Using Locally Developed Crop Coefficients against Satellite-Derived Crop Evapotranspiration in a Semiarid Climate

Koffi Djaman [1,*], Ali T. Mohammed [2] and Komlan Koudahe [3]

[1] Department of Plant and Environmental Sciences, New Mexico State University, Agricultural Science Center at Farmington, 300 County Road 4063, Farmington, NM 87499, USA
[2] Department of Biological Systems Engineering, University of Nebraska-Lincoln, Lincoln, NE 68583, USA; amohammed2@unl.edu
[3] Department of Biosystems Engineering, University of Manitoba, 75 Chancellors Circle, Winnipeg, MB R3T 5V6, Canada; koudahek@myumanitoba.ca
* Correspondence: kdjaman@nmsu.edu; Tel.: +1-505-960-7757

Abstract: Actual crop evapotranspiration (ETa) is measured or estimated using different methods, and its accuracy is critical for water management under precision agriculture. The objective of this study was to compare maize ETa estimated by the two-step approach using a locally developed crop coefficient curve with satellite-retrieved evapotranspiration by six models incorporated in the OpenET to identify the best evapotranspiration estimation alternatives to the two-step approach for water management in northern New Mexico. Maize (*Zea mays* L.) was planted at the NMSU Agricultural Science Center at Farmington from 2017 to 2022 and uniformly managed across years. Water management in plants was based on maize's actual evapotranspiration estimated as the product of the reference evapotranspiration and the local crop coefficient, which is described as a third-order polynomial function of the accumulated heat units by maize plants. For the same growing seasons, maize ETa was retrieved from satellite, and was estimated by six models listed within the OpenET from 2017 to 2022. The results show that maize daily ETa was consistently smaller when measured by SIMS and PT-JPL during maize initial and actively growing stages, while ETc(kc), SIMS and eeMETRIC showed similar maize daily ETa during maize full canopy development and mid-season, and which overcome the evapotranspiration estimated by DisALEXI, PT-JPL, geeSEBAL, and SSBop. ETc(kc) drastically dropped and became the lowest value among all ETa estimation models after the first fall snow or the first killing frost. Regarding the seasonal average, all six models included in OpenET showed smaller maize evapotranspiration. Maize seasonal evapotranspiration varied from 589.7 to 683.2 mm. eeMETRIC compares most similarly to the ETc(kc) model, followed by SIMS, with percent errors of 2.58 and 7.74% on a daily basis and 2.43 and 7.88% on a seasonal basis, with the lowest MBE and RMSE values, respectively, and could be used as an alternative for maize actual daily evapotranspiration for water management in northern New Mexico. The results of this study could be used by water managers and crop growers to improve water management in the Four Corners region, using eeMETRIC for crop water use to improve water management and conservation under sustainable agriculture.

Keywords: crop evapotranspiration; crop coefficients; remote sensing; OpenET; maize

Citation: Djaman, K.; Mohammed, A.T.; Koudahe, K. Accuracy of Estimated Crop Evapotranspiration Using Locally Developed Crop Coefficients against Satellite-Derived Crop Evapotranspiration in a Semiarid Climate. *Agronomy* **2023**, *13*, 1937. https://doi.org/10.3390/agronomy13071937

Academic Editor: Junliang Fan

Received: 5 June 2023
Revised: 7 July 2023
Accepted: 20 July 2023
Published: 22 July 2023

1. Introduction

Producing a sufficient amount of food, fiber, and fuel under water-limiting conditions has been a longstanding challenge, especially when coupled with the rapidly growing population and climate change, and their negative impacts on water resources. Climate change raises temperatures coupled with natural fluctuations in precipitation, resulting in decreases in soil moisture content [1,2]. There are increases in air temperature and tremendous alterations in annual and crop growing season precipitation causing frequent droughts, floods, and heat waves under the changing climate [3]. These changes hardly impact crop production. The accurate estimation of crop water use is critical mostly under semiarid and arid climatic conditions for improving farm water management and crop water use efficiency [4,5]. The United States is impacted by decreasing irrigation water availability in many regions, including the southwestern United States, which mostly affects agriculture production fields due to the high-water demand in the southwestern area.

Developing and evaluating accurate actual crop evapotranspiration (ETa) measurement/estimate methods is important to providing real-time ETa for irrigation water management to farmers and water managers and allowing for the calculation of irrigation use efficiency indices. Moreover, to develop criteria for in-season water management, long-term estimates of water supply, demand, and use are important. Crop evapotranspiration estimation and measurement have been improved using the two-step approach [6], lysimeters [7,8], the Eddy covariance system [9,10], the Bowen Energy Balance Ratio [10–13], sap flow [14], and scintillometers [15–17]; however, the measurement is limited to a certain spatial extent.

Remote sensing is an indirect approach to estimating Eta and has become increasingly common. It has the potential to revolutionize the methodology of ETa estimation. It is a function of mathematical equations that convert the measured satellite radiances into an estimate of ETa [18]. Well-documented progress in evapotranspiration estimation has been made through the last few decades by combining the use of satellite remote sensing data from optical and thermal infrared sensors [19–22]. Remote sensing offers a better capacity to estimate crop evapotranspiration over a large area or region [23–26]; however, this method faces the challenge of the complexity of the required algorithms to account for complex spatiotemporal variations, and the intensive computation of the complex evapotranspiration models due to the large quantity and file sizes of satellite images and associated weather variables [26]. Many remote sensing models are available to estimate ETa, such as the Surface Energy Balance Index [27], the Simplified Surface Energy Balance Index [28], the Surface Energy Balance System [29], the Surface Energy Balance Algorithm for Land (SEBAL) [18] and OpenET [30]. While each one has its specifications, there are common requirements of specialized instrumentation, knowledge, accuracy, accessibility, and cost/time efficiency.

OpenET is a satellite-based tool for mapping evapotranspiration estimates from a web platform at a field scale of 30 m on daily, monthly, and annual bases (www.openetdata.org, accessed on 16 February 2022), and it has been developed by several scientists (30+) from various US institutes [31]. A large dataset of ground-based evapotranspiration (i.e., 194 stations in the US) was developed to provide a consistent reference to support the evaluation of the OpenET satellite-based remote sensing evapotranspiration for a wide range of applications related to irrigation water resources management at the field to watershed scales [32]. An evaluation study was conducted to evaluate the National Water Model's Evapotranspiration (NWM) fluxes against OpenET products from 2016 to 2020 for different months and seasons by Nassar et al. [33]. They found that for the entire watershed, comparisons are much more consistent, but indicate that the NWM tends to underpredict evapotranspiration fluxes, particularly from June to December.

New Mexico is one of the more arid states in the US, and is prone to drought and warmer growing seasons [34]. Other studies, such as that by Prein et al. [35], reported that the frequent weather type changes in the Southwest resulted in a significant precipitation decrease. Smith and Katz [36] reported that the southwestern region has lost more than USD 100 billion since 2000 due to a series of droughts [37]. Consequently, studies have reported a considerable increase in daily/seasonal actual evapotranspiration (ETa) demand due to a combination of factors, including relatively low seasonal rainfall and high temperatures, combined with high wind velocity [38,39]. ETa data are vital for the management of water resources and maximizing crop water productivity, advancing water management strategies, and sustaining water supplies for agriculture in the Southwest. ETa is also considered the second largest component of surface water after precipitation [40].

The northwest of New Mexico is characterized by a semiarid/arid climate with a variable annual precipitation, which averaged 237.5 mm for the 1930–2017 period, while precipitation in the crop growing season (May through September) averaged 144.1 mm for the same period, which was concentrated during the July–September monsoon [41]. Pre-irrigation is therefore required before or just after planting, and no crop is produced without irrigation in northwest New Mexico. Under these limited water resource conditions, irrigation application and management are key factors that could limit crop production in the area. There is a need to accurately estimate crop water use, which should be matched by irrigation in addition to the in-season precipitation. In northwest New Mexico, crop production is one of the main activities of the numerous small stakeholder farmers, in addition to the Navajo Agricultural Products Industry (NAPI), one of the largest agricultural businesses owned and operated by Native Americans in the United States. The NAPI is operating about 36,421 fully developed hectares equipped with irrigation systems, with a total target of 44,770 hectares. The NAPI grows a variety of crops, amongst which a preponderant place is given to maize production.

Maize seasonal actual evapotranspiration varies across different agroclimatic zones, and it is a function of hybrid types, relative maturity date, agronomic practices, and environmental conditions. Djaman et al. [42] reported that seasonal maize ETa ranged from 634.2 to 697.7 mm, averaging 665.3 mm across different ETa estimation methods, in a study in northern New Mexico. Barnes [43] found a seasonal ETa of 684 mm in Farmington, NM, whereas Djaman et al. [42] reported that total maize water requirements ranged from 758.4 to 848.3 mm in a study investigating the impacts of planting dates on the total water requirements in northern New Mexico. Limited water use data exist across northwest New Mexico for maize and other crops, and OpenET might provide a good opportunity for crop growers, university researchers, and crop consultants to improve crop water use in the area. While OpenET offers six different crop evapotranspiration estimates, there are no studies addressing the measured crop evapotranspiration via the OpenET data set for northwestern New Mexico. The objective of this study was to compare maize ETa estimated by the two-step approach using locally developed crop coefficients to satellite-retrieved evapotranspiration composed by six models included in the OpenET so as to identify the model that compares most favorably to the two-step approach for water management in northwest New Mexico.

2. Materials and Methods

2.1. Experimental Site Characteristics for the Study Area

The study was conducted at the Agricultural Experiment Station at Farmington, located in northwestern New Mexico, USA. The geographical coordinates of the site are latitude 36.69′ N, longitude 108.31′ W, and elevation 1720 m. Weather variables were monitored at the station using an automated weather station. Minimum temperature (Tmin), maximum temperature (Tmax), average temperature (Tmean), minimum relative humidity (RHmin), maximum relative humidity (RHmax), average relative humidity (RHmean), wind speed (U_2), and solar radiation (Rs) were collected daily over well-maintained grass by an automated weather station installed at the site by the New Mexico Climate Center. The soil at this site is a fine sandy loam soil with some small patches of Avalon sandy loam and Doak loam. Soil moisture at field capacity varies from 29.7 to 32.5%, and the soil moisture content at wilting point is about 16%. The organic matter content of the soil is less than 1% and the soil pH varies between 7.8 and 8.3.

2.2. Crop Management

Maize was planted at the experiment site for the 2017–2022 period and managed under full irrigation via a center pivot sprinkler irrigation system. The research station adopted a specific crop rotation among six center pivots available at the station. After field disking and harrowing, the plot was pre-irrigated as there was no rainfall before planting and the residual soil moisture is usually too low to allow seed germination. Maize was planted on 15 May 2017; 25 May 2018; 17 May 2019; 13 May 2020; 19 May 2021; and 26 May 2022. Nitrogen, phosphorus, and potassium fertilizer application rates were based on the NMSU recommendations, and were 269, 232, 345, 323, 309, and 284 kg/ha for nitrogen, 60, 84, 56, 112, 59 and 40 kg/ha for P_2O_5, and 76, 92, 84, 101, 86, and 60 kg/ha for K_2O during the maize 2017, 2018, 2019, 2020, 2021, and 2022 growing seasons, respectively. The field was fully irrigated through a central pivot irrigation system to avoid any impact of water stress on crop growth, development, and grain yield. Irrigation scheduling was based on evapotranspiration, and the depletion criterion of 40% to 45% total available water was practiced, preventing the plants from experiencing any water stress, as the center pivot requires one to two days to complete a full revolution. The crops were harvested usually in November–December depending on the equipment and the personnel's availability, and the harvest dates are not considered in the present study. For the study period, crop ETa estimation stopped on October 15 as irrigation water goes off and the killing frost usually occurs at the beginning of October [44]. Maize plots were managed similarly across years and the applied fertilizer rates were based on soil testing chemical properties at the beginning of each growing season. Plots were kept weed-free by a combination of chemical herbicide application (atrazine, glyphosate) and hand weeding if necessary.

2.3. Irrigation Management

Irrigation scheduling was based on crop actual evapotranspiration [42]. Maize's actual evapotranspiration was estimated according to the equation proposed by Jenson [6] and Allen et al. [7].

$$ETa = Kc \times ETo \tag{1}$$

where ETa = daily actual evapotranspiration (mm), Kc = daily crop coefficient, ETo = grass reference evapotranspiration (mm).

The daily grass reference ET was computed using the standardized ASCE form of the Penman–Monteith (PM-ETo) Equation (2):

$$ETo = \frac{0.408\Delta(Rn - G) + (\gamma Cn\ u2/(T + 273))(es - ea)}{\Delta + \gamma(1 + Cd\ u2)} \tag{2}$$

where ETo is the reference evapotranspiration (mm day^{-1}), Δ is the slope of saturation vapor pressure versus air temperature curve (kPa °C^{-1}), Rn is the net radiation at the crop surface (MJ m^{-2} d^{-1}), G is the soil heat flux density at the soil surface (MJ m^{-2} d^{-1}), T is the mean daily air temperature at 2 m height (°C), $u2$ is the mean daily wind speed at 2 m height (m s^{-1}), es is the saturation vapor pressure at 2 m height (kPa), ea is the actual vapor pressure at 2 m height (kPa), $es - ea$ is the saturation vapor pressure deficit (kPa), γ is the psychrometric constant (kPa °C^{-1}), and Cn and Cd are constants with values of 900 °C mm s^3 Mg^{-1} d^{-1} and 0.34 s m^{-1}. The procedure developed by Allen et al. [7] was used to compute the parameters Δ, Rn, G, es, and ea.

For the present study, a crop coefficient curve locally developed by Sammis et al. [45] for the study site was used. Sammis et al. [45] grew maize in non-weighing lysimeters across different locations in New Mexico and Penman–Monteith estimated the reference evapotranspiration to determine maize crop coefficient as a function of the accumulated thermal unit from planting to crop physiological maturity. To generate the Kc curve, maize thermal units were estimated for each growing season, and the third-order polynomial equation developed by Sammis et al. [45] was applied daily.

$$Kc = 0.12 + 0.00168 \times TU - 2.46 \times 10^{-7} \times TU^2 - 4.37 \times 10^{-10} \times TU^3 \tag{3}$$

where Kc is the daily crop coefficient and TU is the thermal unit (°C).

The thermal unit is the accumulation of the growing degree days (GDD), which is a cumulative temperature that contributes to plant growth and development during the growing season, and is expressed as follows:

$$TU = \sum_{i=1}^{n} \frac{Tmax + Tmin}{2} - Tbase \tag{4}$$

where TU = thermal unit (°C), $Tmax$ = maximum air temperature (°C), $Tmin$ = minimum air temperature (°C), $Tbase$ = base temperature threshold for maize (10 °C), and n = number of days. The base temperature for calculating growing degree days is the minimum threshold temperature at which plant growth starts. The maximum and minimum temperature thresholds of 30 °C and 10 °C, respectively, were used. All temperature values exceeding the threshold were reduced to 30 °C, and values below 10 °C were taken as 10 °C because no growth occurs above or below the threshold (base) temperature values. If the average daily temperature was below the base temperature, the TU value was assumed to be zero.

2.4. Satellite-Derived Crop Actual Evapotranspiration

Maize daily actual evapotranspiration was retrieved from the OpenET (https://openetdata.org/, accessed on 4 January 2023), [31]. The maize plot was selected each year from 2017 to 2022 at the Agricultural Science Center at Farmington using the OpenET website (Figure 1). The studied models within the OpenET are as follow: ALEXI/DisALEXI is Atmosphere–Land Exchange Inverse/Disaggregation of the Atmosphere–Land Exchange Inverse (ver. 0.0.27) [46,47], eeMETRIC is Mapping Evapotranspiration at High Resolution with Internalized Calibration (ver. 0.20.15) [48–50], geeSEBAL is Surface Energy Balance Algorithm for Land using Google Earth Engine (ver. 0.2.1) [18,51], PT-JPL is Priestley–Taylor Jet Propulsion Laboratory (ver. 0.2.1) [52], SIMS is Satellite Irrigation Management Support (ver. 0.0.20) [30,53], and SSEBop is Operational Simplified Surface Energy Balance (ver 0.1.5) [54,55]. In all openET models except ALEXI-DisALEXI, ETo data are used in the estimation of daily actual evapotranspiration between Landsat satellite overpasses every eight days. For each satellite overpass date, a fraction of grass reference evapotranspiration (EToF) for each 30 m pixel is estimated as a ratio between the satellite-derived evapotranspiration by the ETo. The EToF values are then linearly interpolated for days between satellite overpasses. Next, the interpolated fraction is multiplied by the corresponding daily ETo values resulting in daily actual evapotranspiration values for each pixel, which are then combined into monthly and annual periods. On the other hand, ALEXI/DisALEXI relies on the coarser-resolution ET information from the ALEXI model [46] with GOES satellite information to produce the daily ET. The coarser-resolution evapotranspiration values are disaggregated to 30 m using the DisALEXI algorithm [56]. Daily actual evapotranspiration values given by all six models and the ensemble average were retrieved for the maize plot from planting to 15 October every season for the period of 2017–2022.

2.5. Data and Statistical Analysis

Daily actual evapotranspiration data were plotted and compared against each other. All six growing seasons' data from the OpenET were combined and plotted against the locally developed Kc curve ETa and the simple linear regression slope and coefficient of determination were used to appreciate the quality of the fitness of the satellite-derived ETa against the locally developed Kc curve ETa. The CoStat software was used for data analysis [57]. The Kolmogorov–Smirnov test was performed to check the normal distribution of the dataset time series and the Mann–Whitney U tests were used for means comparison. The percent error (PE), mean bias error (MBE), and root mean squared error (RMSE) were also used for model evaluation.

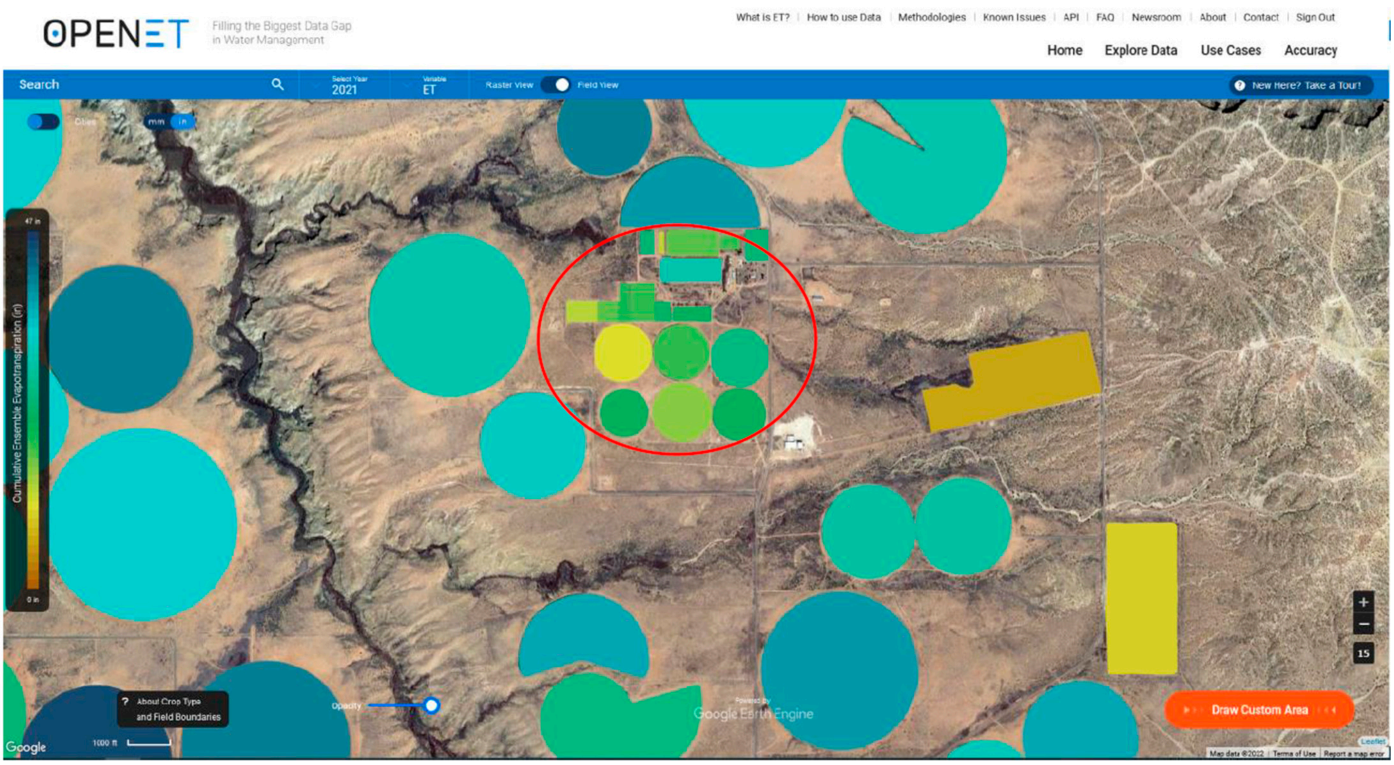

Figure 1. The OpenET Data Explorer showing the NMSU Agricultural Center at Farmington (within the red circle). The circles are fields irrigated with center pivot system.

3. Results and Discussion

3.1. Weather Conditions during the Study Period

The 2017–2022 period daily weather conditions are presented in Figures 2 and 3. The maximum, minimum, and average temperatures increased from January to the maximum values in mid-July and decreased thereafter to the minimum values at the end of December of each year. Tmax varied from −9.3 to 38.0 °C; Tmin varied from −21.6 to 21.8 °C, and Tmean varied from −14.9 °C to 29.4 °C (Figure 2a). The minima of Tmax, Tmin, and Tmean occurred in late December, and the maxima occurred in July of each year. The annual Tmax, Tmin, and Tmean averages were 20.2, 4.1, and 12.1 °C, respectively. The air maximum relative humidity RHmax varied from 18.3% to 100%, the RHmin varied from 0% to 83.2%, and the RHmean varied from 9.9% to 95.5% (Figure 2b); they averaged 71.6, 21.2, and 43.6%, respectively, for the 2017–2022 period. Daily precipitation varied from 0 to 19.1 mm and averaged 0.4 mm, and the annual total precipitation averaged 140.6 mm for the 2017–2022 period (Figure 2c). The daily average wind speed fluctuated considerably, and varied from 0.5 to 7.6 m/s, averaging 2.2 m/s for the study period. The highest wind speed values were observed in the spring of each year, as shown in Figure 3a. The daily solar radiation varied from 2.1 to 32.3 MJ/m^2 and averaged 18.8 MJ/m^2 (Figure 3a). Daily maize growing day temperatures varied from 0 to 19.5 °C, showing that maize planting could start as early as early April (Figure 3b), and the annual total thermal unit for maize varied from 1666.8 to 1933.5 °C, and averaged 1832.2 °C for the 2017–2022 period (Figure 3b).

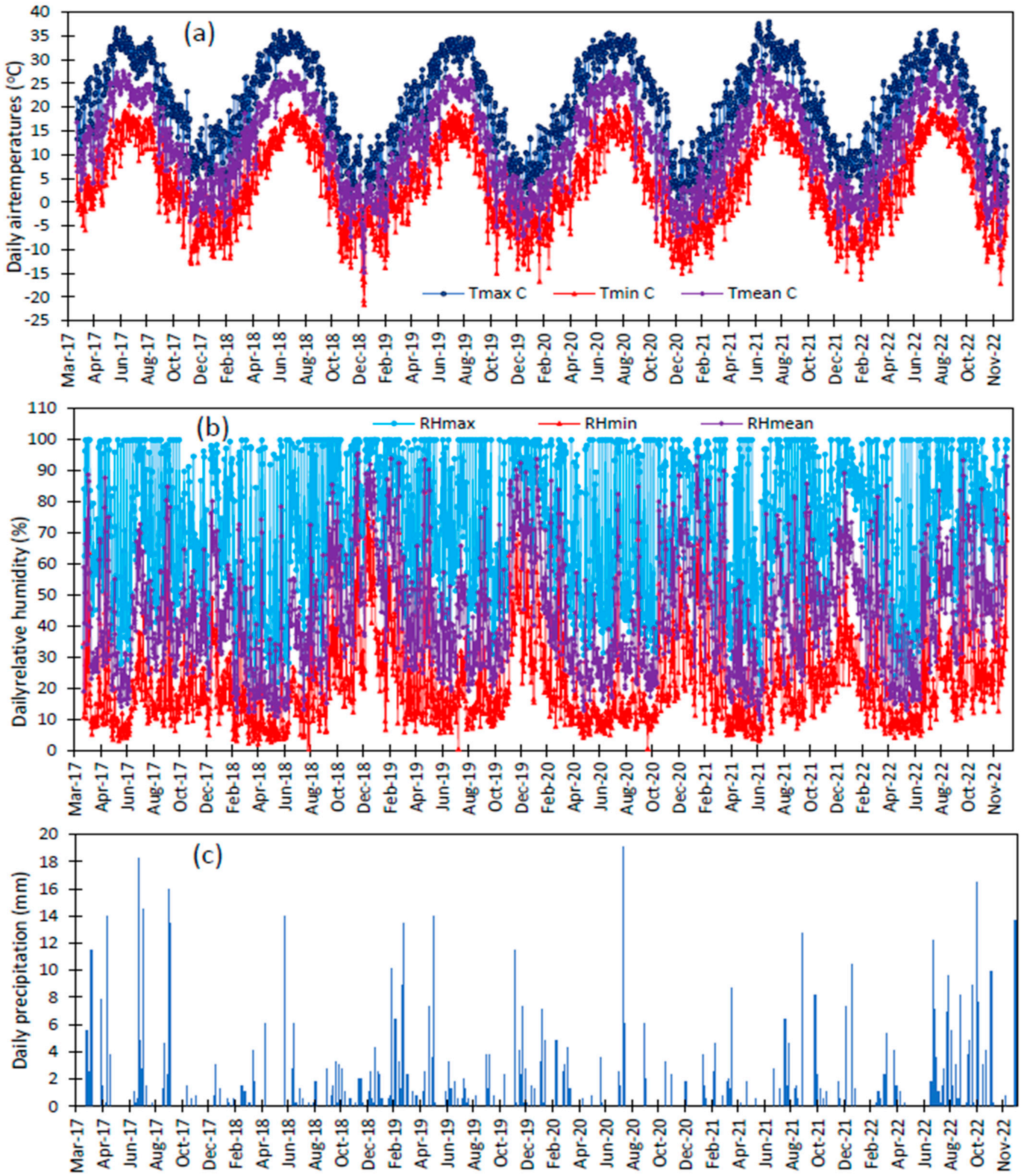

Figure 2. Dynamics of (**a**) air maximum temperature (Tmax), minimum temperature (Tmin) and average temperature (Tmean), (**b**) air maximum relative humidity (RHmax), minimum relative humidity (RHmin), and average relative humidity (RHmean), and (**c**) daily precipitation during the 2017–2022 period.

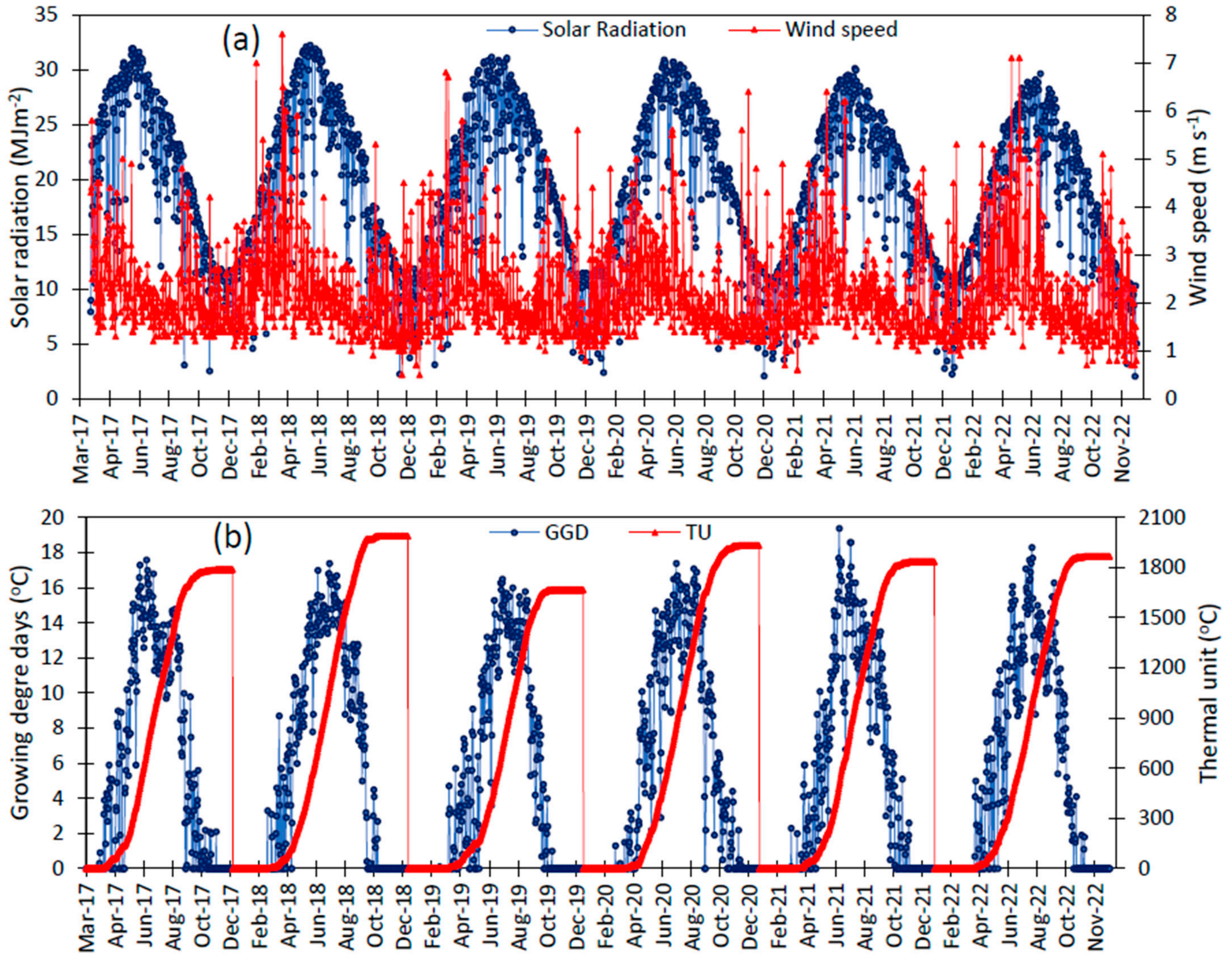

Figure 3. Dynamics of (**a**) solar radiation and wind speed, and (**b**) the growing degree days and the thermal unit during the 2017–2022 period.

3.2. Maize Daily Actual Evapotranspiration

The maize daily actual evapotranspiration estimated by the seven models is presented in Figure 4. The daily ETa varied from 0.4 to 8.9 mm in 2017, from 0.4 to 9.2 mm in 2018, from 0.3 to 8.2 mm in 2019, from 0.3 to 8.9 mm in 2020, from 0.5 to 8.4 mm in 2021, and from 0.6 to 8.6 mm in 2022, and averaged 4.1, 4.4, 4.2, 4.4, 4.2, and 4.1 mm/day during the respective growing seasons. All seven models showed a similar trend in maize daily evapotranspiration, which increased from planting to full development (July–August) and decreased thereafter toward the crop physiological maturity stage with plant senescence. Assuming that the maize actual evapotranspiration estimated by the locally developed Kc is the accurate one, the geeSEBAL, DisALEXIS, eeMETRIC, and SSEBop models showed larger maize daily evapotranspiration during the maize initial state, while the other models showed smaller maize evapotranspiration (Figure 4). All models showed smaller maize evapotranspiration during the mid-season, with the SIMS and eeMETRIC being the closest to the ETc(kc), while all models showed larger maize daily evapotranspiration during the late season (Figure 4). Considering the growing season, all OpenET models showed smaller maize evapotranspiration for the 2017–2022 period with average PE values from −24.87 to −2.58% (Table 1), and also an MBE that varied from −1.05 to 0.11 mm/day (Table 2). Seasonal RMSE varied from 1.25 to 1.70 mm/day (Table 3). Overall, eeMETRIC was the most accurate model included in the OpenET, followed by SIMS (Tables 1–3), and could be considered for maize ET retrieval in the absence of onsite measurement or the estimation of maize daily evapotranspiration. The regression between the ETc(kc)-estimated ETa and those of the six other ETa models in OpenET is presented in Figure 5. The regression slope varied from 0.7029 to 0.9004, and the coefficient of determination ranged from 0.9048 to 0.9279 (Figure 5). Combining all statistical parameters, eeMETRIC and SIMS compare most favorably to the ETc(kc) for maize evapotranspiration estimation in northwest New Mexico.

Table 1. Percent error (%) of modeled maize evapotranspiration (ET) for the 2017–2022 period.

Seasons	Ensemble	eeMETRIC	SSEBop	SIMS	PT-JPL	DisALEXI	geeSEBAL
2017	−5.14	0.66	−4.14	−8.56	−17.58	−10.78	−3.23
2018	−40.06	−7.36	−20.89	−9.70	−25.39	−24.82	−16.20
2019	−15.95	−8.29	−7.04	−6.97	−23.82	−16.97	−13.51
2020	−4.62	9.69	0.30	−12.90	−38.28	−5.30	−4.81
2021	−16.97	−6.01	−21.93	−6.78	−26.03	−14.91	−14.39
2022	−11.74	−4.18	−24.36	−1.50	−18.14	−10.73	−13.05
Average	−15.75	−2.58	−13.01	−7.74	−24.87	−13.92	−10.86

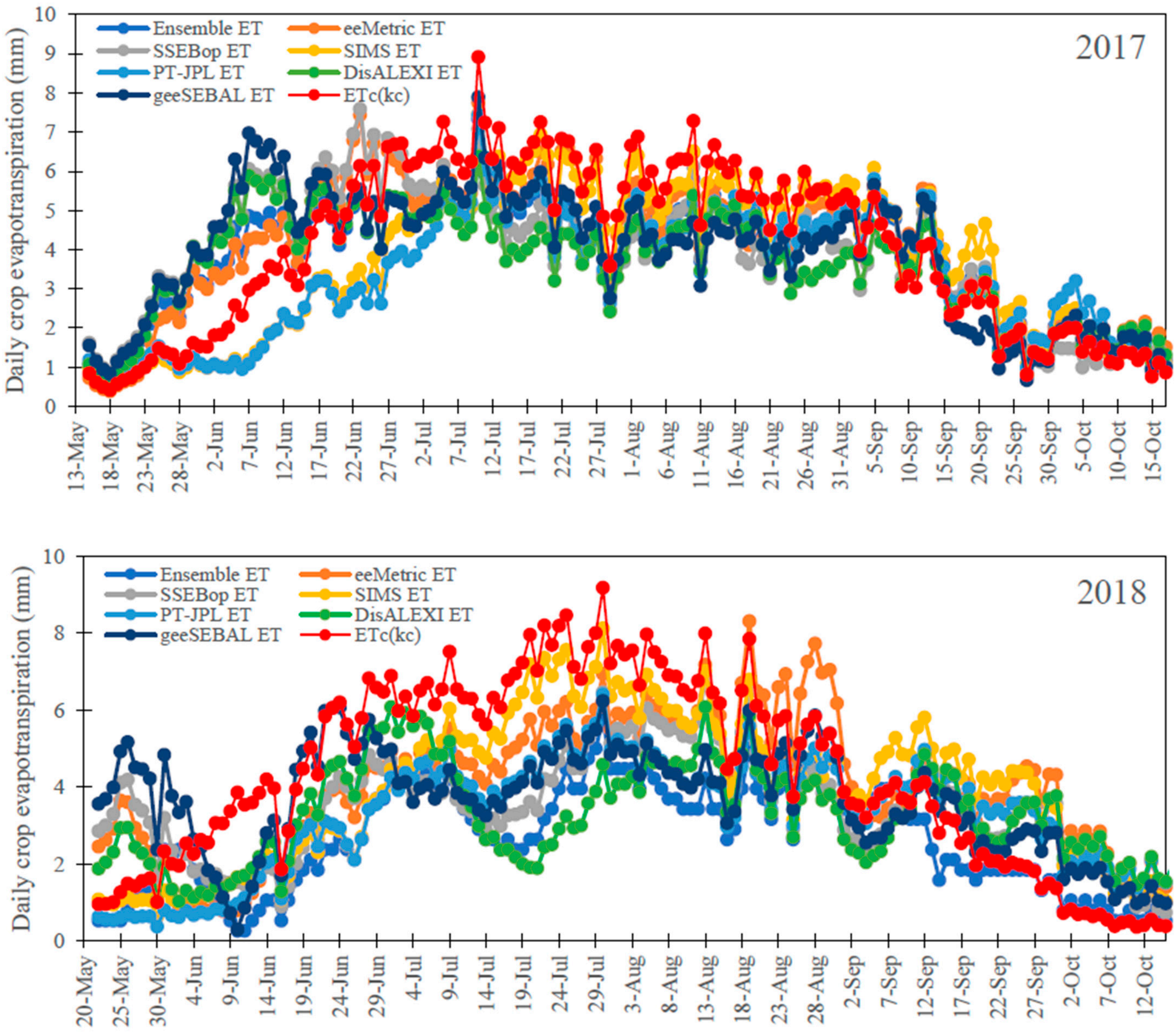

Figure 4. *Cont.*

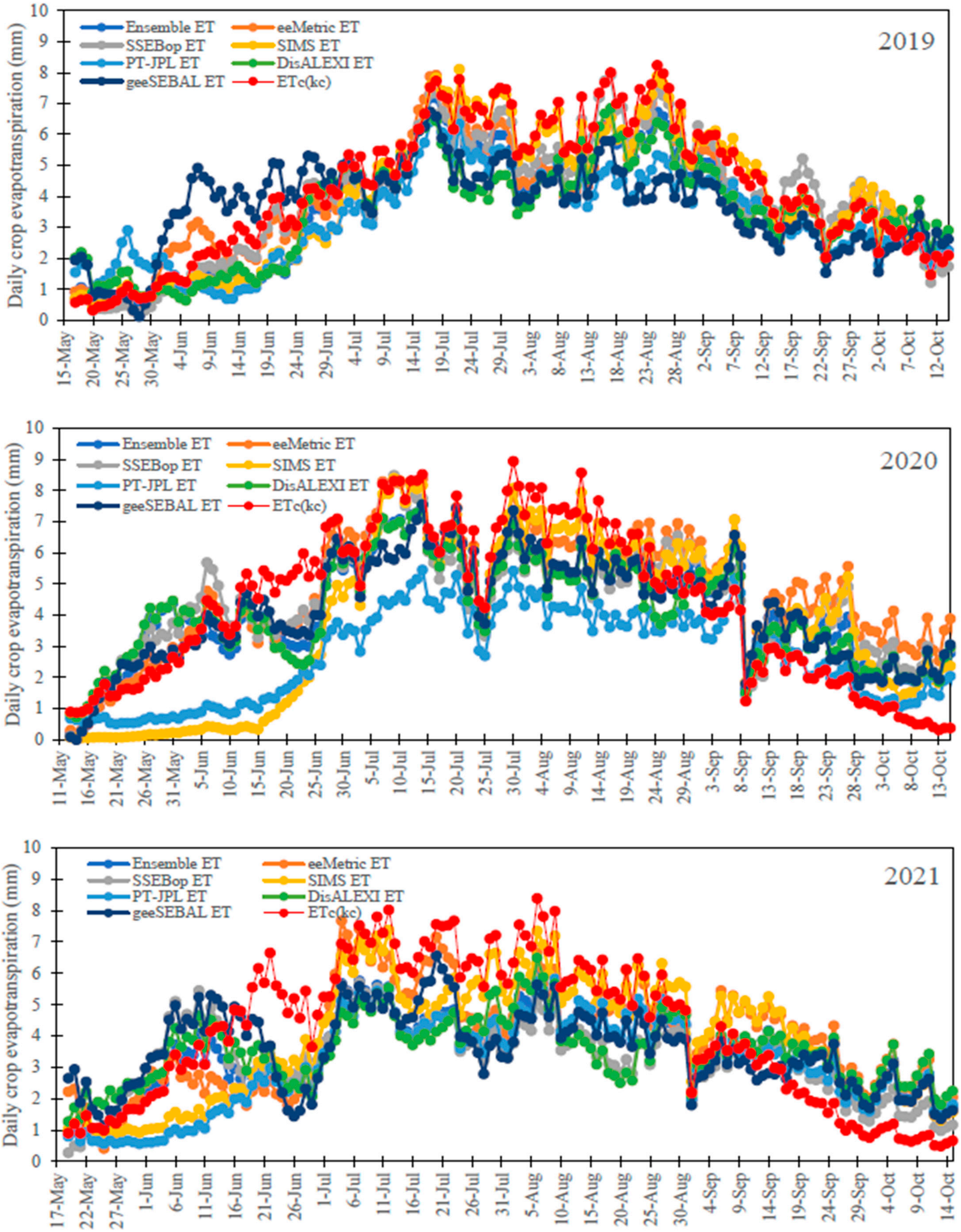

Figure 4. *Cont.*

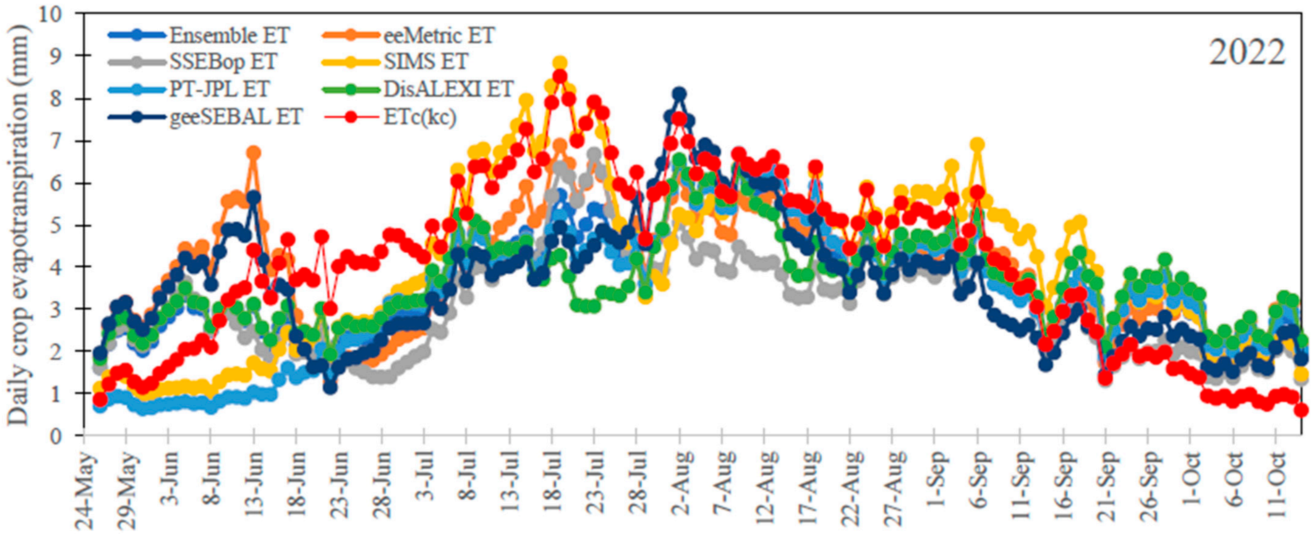

Figure 4. Dynamics of maize daily evapotranspiration estimated for different models during the 2017–2022 period.

Table 2. Mean bias error (mm/day) of modeled maize evapotranspiration (ET) for the 2017–2022 period.

Seasons	Ensemble	eeMETRIC	SSEBop	SIMS	PT-JPL	DisALEXI	geeSEBAL
2017	−0.21	0.03	−0.17	−0.35	−0.72	−0.44	−0.13
2018	−1.74	−0.32	−0.91	−0.42	−1.11	−1.08	−0.70
2019	−0.68	−0.35	−0.30	−0.30	−1.01	−0.72	−0.57
2020	−0.20	0.42	0.01	−0.56	−1.68	−0.23	−0.21
2021	−0.71	−0.25	−0.91	−0.28	−1.08	−0.62	−0.60
2022	−0.48	−0.17	−1.00	−0.06	−0.75	−0.44	−0.54
Average	−0.67	−0.11	−0.55	−0.33	−1.06	−0.59	−0.46

Table 3. Root mean squared error (mm/day) of modeled maize evapotranspiration (ET) for the 2017–2022 period.

Seasons	Ensemble	eeMETRIC	SSEBop	SIMS	PT-JPL	DisALEXI	geeSEBAL
2017	1.00	0.80	1.35	0.95	1.27	1.46	1.39
2018	2.30	1.63	1.85	1.45	1.91	2.19	1.85
2019	0.94	0.73	0.58	0.69	1.43	1.21	1.51
2020	1.30	1.41	1.32	1.91	2.27	1.34	1.16
2021	1.58	1.53	1.74	1.32	1.78	1.76	1.65
2022	1.30	1.39	1.62	1.11	1.53	1.62	1.53
Average	1.40	1.25	1.41	1.24	1.70	1.60	1.52

Maize evapotranspiration estimated by the SSEBop model was significantly similar to the locally developed evapotranspiration for three years over six (Table 4). The findings do not agree with those of Senay et al. [26], who found that crop evapotranspiration estimated with the SSEBop model was stronger, with an R^2 value of 0.82, an RMSE of 0.97 mm/day, and average bias of 12%, with crop evapotranspiration measured with the Eddy covariance system over croplands. Relatively good correspondence (R^2 up to 0.88, RMSE as low as 0.5 mm/day) was found between SSEBop evapotranspiration estimates and gridded-flux data and water balance evapotranspiration approaches in the southwest United States [58]. In another study, Senay et al. [59] found that SSEBop model-estimated crop water use, when compared with the eddy-covariance flux towers dataset, showed strong correspondence, with an R^2 greater than 0.80 and RMSE values ranging from 0.2 to 0.63 mm/day across the upper Rio Grande Basin for the 1986–2015 period. The results gave significantly different evapotranspiration estimates compared to the local kc evapotranspiration estimated for 4 years over 6 (Table 5). These results agree with those of de Oliveira et al. [60], who found that evapotranspiration estimated using the SEBAL showed higher differences in relation to the observed values. In contrast, Kaysert et al. [61] reported that daily estimates of geeSEBAL yielded an average RMSD of 0.91 mm/day when compared to eddy covariance system data, while Gonçalves et al. [62] indicated that geeSEBAL has significant potential for use in the assessment of crop evapotranspiration for irrigation monitoring and management in Brazil, even in areas with missing climate data. The applicability of the SEBAL model for paddy field evapotranspiration estimation was evaluated for the 2000–2017 period in Jiangxi Province (south of the Yangtze River), China, and the results show that the SEBAL model estimated crop evapotranspiration accurately on a daily scale, with R^2 and RMSE values of 0.85 and 0.84 mm/day, respectively [63]. This study showed the applicability of the SEBAL model in paddy fields in subtropical regions and provided a basis and reference for the rational allocation of water resources at a regional scale [63].

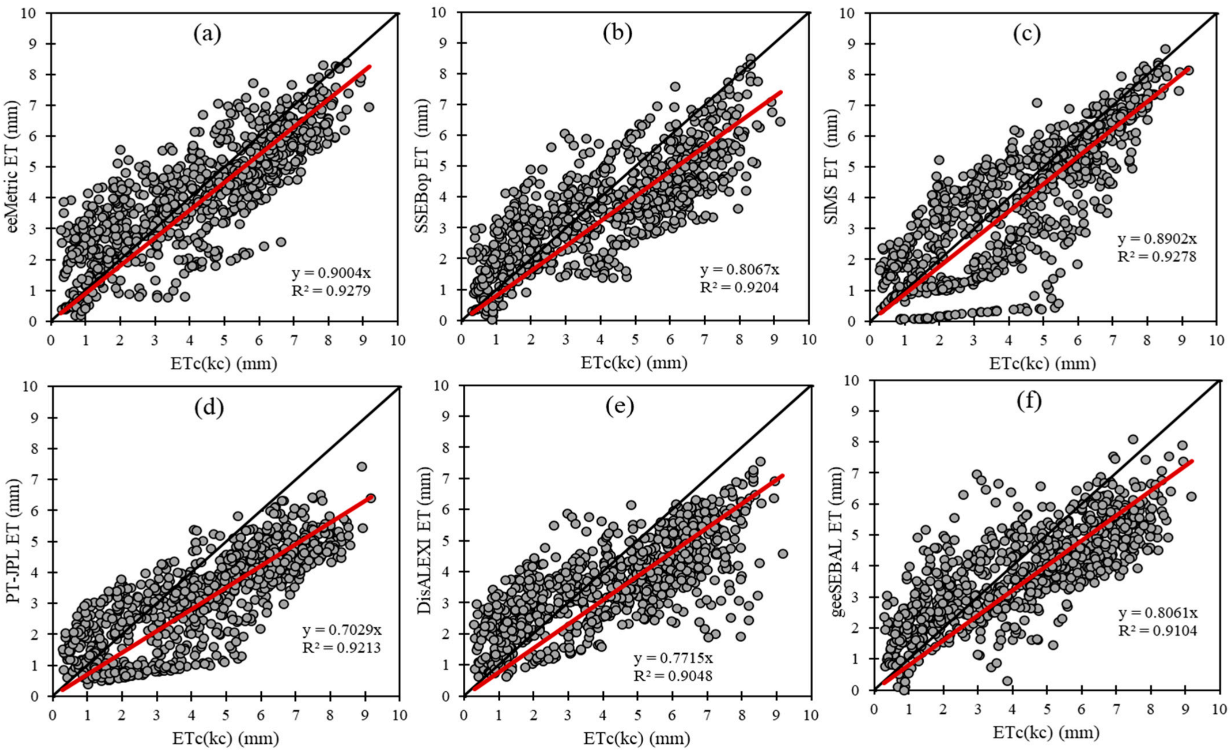

Figure 5. Relationship between the crop coefficient-modeled evapotranspiration (ETc) and the different models in the OpenET platform, (**a**) eeMETRIC vs. ETc(kc) (**b**) SSEBop vs. ETc(kc) (**c**) SIMS vs. ETc(kc) (**d**) PT-JPL vs. ETc(kc) (**e**) DisALEXI vs. ETc(kc) (**f**) geeSEBAL vs. ETc(kc).

Table 4. Summary of the Kolmogorov–Smirnov test comparing the distribution of the daily evapotranspiration (ET) estimated by the seven ET models.

Years	Parameters	eeMETRIC	SSEBop	SIMS	PT-JPL	DisALEXI	geeSEBAL	ETc(kc)
2017	Count	154	154	154	154	154	154	154
	Mean	4.102	3.906	3.726	3.359	3.636	3.943	4.075
	Median	4.568	4.121	4.255	3.594	3.931	4.293	4.521
	Standard Deviation	1.755	1.623	1.913	1.582	1.364	1.621	2.133
	Skewness	−0.460	−0.268	−0.200	−0.102	−0.485	−0.359	−0.166
	Kurtosis	−0.793	−0.662	−1.383	−1.154	−0.689	−0.799	−1.324
	K-S test statistic (D)	0.116	0.100	0.130	0.107	0.096	0.127	0.121
	p-value	0.029	0.083	0.010	0.054	0.108	0.013	0.020
	Significance	DNND	DND	DNND	DND	DND	DNND	DNND

Table 4. *Cont.*

Years	Parameters	eeMETRIC	SSEBop	SIMS	PT-JPL	DisALEXI	geeSEBAL	ETc(kc)
2018	Count	147	147	147	147	147	147	147
	Mean	4.031	3.443	3.930	3.247	3.272	3.647	4.352
	Median	4.253	3.409	4.234	3.587	3.196	3.825	4.193
	Standard Deviation	1.761	1.351	1.946	1.480	1.269	1.366	2.417
	Skewness	−0.094	0.087	−0.048	−0.433	0.243	−0.374	−0.092
	Kurtosis	−0.670	−0.497	−1.114	−0.886	−0.799	−0.629	−1.255
	K-S test statistic (D)	0.056	0.051	0.098	0.109	0.094	0.063	0.123
	p-value	0.717	0.828	0.113	0.055	0.140	0.591	0.022
	Significance	DND	DND	DND	DND	DND	DND	DNND
2019	Count	152	152	152	152	152	152	152
	Mean	3.889	3.943	3.945	3.231	3.521	3.668	4.241
	Median	3.730	4.211	3.926	3.027	3.659	3.912	4.215
	Standard Deviation	1.867	2.038	2.186	1.458	1.626	1.371	2.171
	Skewness	0.040	−0.173	0.036	0.125	−0.100	−0.481	−0.038
	Kurtosis	−0.618	−0.922	−1.248	−0.919	−0.914	−0.131	−1.095
	K-S test statistic (D)	0.050	0.068	0.089	0.072	0.093	0.097	0.073
	p-value	0.824	0.455	0.173	0.396	0.135	0.104	0.374
	Significance	DND	DND	DND	DND	DND	DND	DND
2020	Count	156	156	156	156	156	156	156
	Mean	4.804	4.393	3.814	2.703	4.147	4.169	4.379
	Median	4.795	4.457	4.114	2.806	3.976	4.200	4.743
	Standard Deviation	1.933	1.716	2.654	1.496	1.602	1.698	2.480
	Skewness	−0.260	−0.078	−0.081	0.001	0.027	−0.183	−0.028
	Kurtosis	−0.646	−0.104	−1.399	−1.431	−0.917	−0.786	−1.289
	K-S test statistic (D)	0.107	0.062	0.118	0.127	0.074	0.088	0.110
	p-value	0.053	0.573	0.024	0.012	0.346	0.168	0.043
	Significance	DND	DND	DNND	DNND	DND	DND	DNND
2021	Count	150	150	150	150	150	150	150
	Mean	3.914	3.251	3.882	3.080	3.544	3.565	4.164
	Median	4.065	3.361	4.177	3.152	3.639	3.628	4.451
	Standard Deviation	1.662	1.249	1.904	1.474	1.047	1.234	2.304
	Skewness	0.130	−0.318	−0.090	−0.177	0.187	0.040	−0.094
	Kurtosis	−0.851	−0.492	−1.262	−1.092	−0.336	−0.831	−1.315
	K-S test statistic (D)	0.104	0.057	0.116	0.075	0.049	0.059	0.101
	p-value	0.075	0.685	0.032	0.356	0.849	0.653	0.089
	Significance	DND	DND	DNND	DND	DND	DND	DND
2022	Count	143	143	143	143	143	143	143
	Mean	3.951	3.119	4.062	3.376	3.681	3.585	4.123
	Median	4.077	3.112	4.231	3.433	3.533	3.523	4.385
	Standard Deviation	1.333	1.242	1.998	1.584	1.045	1.463	2.077
	Skewness	0.009	0.515	0.146	−0.136	0.596	0.708	−0.097
	Kurtosis	−1.023	−0.266	−1.010	−0.876	−0.174	0.152	−1.097
	K-S test statistic (D)	0.091	0.097	0.094	0.078	0.074	0.103	0.101
	p-value	0.177	0.124	0.149	0.332	0.393	0.087	0.101
	Significance	DND	DND	DND	DND	DND	DND	DND

DND = data normally distributed; DNND = data not normally distributed.

The percent errors of the six models are within the range of ±10–25% suggested by Melton et al. [31]. Therefore, all six models accurately estimated maize daily evapotranspiration at the study site and could be independently used for water management in maize in northern New Mexico. However, eeMETRIC and SIMET should be considered first for water management and water conservation in maize grown at the study site. The better performance of eeMETRIC is reported in other studies. Kilic et al. [64] reported that crop evapotranspiration estimates by eeMETRIC are similar to the eddy covariance measurement data from more than 100 Ameriflux and USDA research sites in the USA, with a ratio of eeMETRIC-estimated evapotranspiration against measurements that averages 1.03 for agricultural land uses. Ortega-Salazar et al. [65] reported that the error within the METRIC compared to the Eddy covariance-measured data was 4 and 6%. Jaafar et al. [66] demonstrated that the TSEB-PT achieved the lowest performance for sites in warm summer humid continental and hot semi-arid climates, as compared to the Eddy covariance time series data. The worse performance of the PT-JPL model might be due to the difference between the universal values of the P-T coefficient, which is likely to decrease in arid environments with natural vegetation and increase in areas with advection similar to that in northern New Mexico [67,68]. In addition, it could be due to the soil evaporation components' formulation, which significantly deviated from the measured values in comparison to crop transpiration [69]. Furthermore, PT-JPL integrates some physically based functions that serve a wide range of hydro-meteorological conditions that are not specific to agroecosystems [70]. The good performance of the SIMS model might be due to its basic features, as it is a reflectance-based model implementing parts of the FAO-56 dual crop coefficient model [7] and combining remotely sensed vegetation parameters and spatially resolved crop type information [71], and it has been shown to be useful in producing accurate evapotranspiration estimates for irrigated agriculture in the Western United States [31,53]. Srivastava et al. [72] evaluated the moderate resolution imaging spectroradiometer (MODIS) satellite-based remote-sensing techniques, and the water-budget approach built into the semidistributed variable infiltration capacity land-surface model, against the two-step approach in the Kangsabati River Basin in eastern India. They found that the water balance method compared most favorably to the two-step approach, while the MODIS-estimated evapotranspiration values were smaller, with a periodic shift that might be attributed to cloud cover and leaf shadowing effects.

Table 5. Summary of the Mann–Whitney U Test comparing the mean of the ET(kc) to the other six ET models.

Years	Parameters	eeMETRIC	SSEBop	SIMS	PT-JPL	DisALEXI	geeSEBAL
2017	The z-score	0.3589	1.2573	1.8433	3.5376	2.4678	1.1549
	p-value	0.3594	0.1038	0.0329	0.0002	0.0068	0.1251
	Significance	n.s.	n.s.	s.	s.	s	n.s.
2018	The z-score	1.26775	3.3697	1.58195	3.93771	3.88009	2.67682
	p-value	0.10204	0.00038	0.05705	0.00004	0.00005	0.00368
	Significance	n.s.	s.	n.s.	s.	s.	s.
2019	The z-score	1.41653	1.12553	1.18034	4.20523	2.84807	2.32348
	p-value	0.0778	0.12924	0.119	0.00001	0.00219	0.01017
	Significance	n.s.	n.s.	n.s.	s.	s.	s.
2020	The z-score	−1.434	0.0295	2.09044	6.17845	0.79513	0.75748
	p-value	0.07636	0.48803	0.01831	0.00001	0.21186	0.22363
	Significance	n.s.	n.s.	s.	s.	n.s.	n.s.
2021	The z-score	1.08153	3.6812	1.15075	4.39468	2.50716	2.5045
	p-value	0.14007	0.00012	0.12507	0.00001	0.00604	0.00621
	Significance	n.s.	s.	n.s.	s.	s.	s.
2022	The z-score	0.9652	4.3141	0.2259	3.3789	2.3351	2.4109
	p-value	0.1660	0.0000	0.4091	0.0004	0.0096	0.0080
	Significance	n.s.	s.	n.s.	s.	s.	s.

n.s. = non significant; s. = signifiant.

3.3. Maize Seasonal Actual Evapotranspiration

Maize seasonal evapotranspiration varied from 589.7 to 683.2 mm and averaged 634.9 mm for the 2017–2022 period (Table 6). The highest seasonal evapotranspiration was obtained in 2020 and the lowest seasonal evapotranspiration was obtained in 2022. OpenET models eeMETRIC, SSEBop, SIMS, PT-JPL, DisALEXI, and geeSEBAL showed smaller maize seasonal evapotranspiration values, by 2.4, 12.7, 7.9, 25.1, 13.9 and 10.8%, respectively. eeMETRIC compares most similarly to the ETc(kc) model, followed by SIMS. These two could be used as alternative sources of maize evapotranspiration for appropriate management in the study area. Maize evapotranspiration for the same research site varied from 634.2 to 697.7 mm, and averaged 665.3 mm, for the 2011–2017 period [42]. Basso and Ritchie [73] reported maize seasonal evapotranspiration values of 640 mm under an arid climate in Arizona. In Nebraska, the fully irrigated maize seasonal evapotranspiration was 620 and 634 mm in 2009 and 2010, respectively [74]. Similar results were obtained by Trout and DeJonge [75] under a semiarid climate in Colorado. In contrast, much higher maize seasonal evapotranspiration (up to 685 mm) in New Mexico has been reported [76], as well as 818 mm [77,78] and 973 mm [79,80] in Texas. While different magnitudes of maize evapotranspiration were reported, the differences might have been due to climatic conditions, the specific evapotranspiration estimation methods, maize hybrids, management practices and other factors.

Table 6. Maize seasonal evapotranspiration (ET) (mm/day) given by the seven models for the 2017–2022 period.

Seasons	Ensemble	eeMETRIC	SSEBop	SIMS	PT-JPL	DisALEXI	geeSEBAL	ETc(kc)
2017	595.3	631.7	601.6	573.8	517.2	559.9	607.3	627.6
2018	383.5	592.6	506.1	577.7	477.3	481.0	536.1	639.7
2019	541.8	591.2	599.3	599.7	491.1	535.2	557.6	644.6
2020	651.6	749.4	685.3	595.0	421.7	646.9	650.3	683.2
2021	518.7	587.1	487.7	582.3	462.1	531.5	534.8	624.7
2022	520.4	565.0	446.0	580.8	482.7	526.4	512.7	589.7
Average	535.2	619.5	554.3	584.9	475.3	546.8	566.5	634.9

4. Conclusions

The six-year data analysis revealed that SIMS and PT-JPL consistently showed lower maize daily evapotranspiration during maize initial and actively growing stages, while ETc(Kc), SIMS, and eeMETRIC showed similar maize daily evapotranspiration during maize full development and reproductive phases. DisALEXI, PT-JPL, geeSEBAL, and SSBop showed the lowest values of maize daily evapotranspiration in the full development and reproductive phases. ETc(kc) drastically dropped, and showed the lowest value among all model estimates, after the first snowfall or the first killing frost. Maize seasonal evapotranspiration varied from 589.7 to 683.2 mm. The eeMETRIC compares most similarly to the ETc(kc) model, followed by SIMS, with percent errors of 2.6 and 7.7% on the daily basis and 2.4 and 7.9% on the seasonal basis, respectively. Both models have the lowest MBE and RMSE values and could be used as an alternative for maize actual daily evapotranspiration for water management in northern New Mexico. For the future direction of our research, direct crop evapotranspiration measurement equipment such as the eddy covariance system could be used for measuring actual crop evapotranspiration for multiple cops and calibrating the six models in OpenET for the study area.

Author Contributions: Conceptualization, K.D.; methodology, K.D. and K.K.; software, K.D.; formal analysis, K.D., A.T.M. and K.K.; resources, K.D.; data curation, K.D., A.T.M. and K.K.; writing—original draft preparation, K.D.; writing—review and editing, K.D., A.T.M. and K.K. All authors have read and agreed to the published version of the manuscript.

Funding: This research received no external funding.

Data Availability Statement: The data will be available on request.

Acknowledgments: We completed this work with the support of New Mexico State University (NMSU) and the Agricultural Science Center at Farmington and all the staff.

Conflicts of Interest: The authors declare no conflict of interest.

References

1. Diffenbaugh, N.S.; Swain, D.L.; Touma, D. Anthropogenic Warming has Increased Drought Risk in California. *Proc. Natl. Acad. Sci. USA* **2015**, *112*, 3931–3936. [CrossRef] [PubMed]
2. Williams, A.P.; Cook, E.R.; Smerdon, J.E.; Cook, B.I.; Abatzoglou, J.T.; Bolles, K.; Baek, S.H.; Badger, A.M.; Livneh, B. Large contribution from anthropogenic warming to an emerging North American megadrought. *Science* **2020**, *368*, 314–318. [CrossRef] [PubMed]

3. IPCC. *Climate Change 2021: The Physical Science Basis. Contribution of Working Group I to the Sixth Assessment Report of the Intergovernmental Panel on Climate Change*; Masson-Delmotte, V., Zhai, P., Pirani, A., Connors, S.L., Pean, C., Berger, S., Caud, N., Chen, Y., Goldfarb, L., Gomis, M.I., et al., Eds.; Cambridge University Press: Cambridge, UK; New York, NY, USA, 2021.
4. Baldocchi, D.; Dralle, D.; Jiang, C.; Ryu, Y. How Much Water Is Evaporated Across California? A Multiyear Assessment Using a Biophysical Model Forced with Satellite Remote Sensing Data. *Water Resour.* **2019**, *55*, 2722–2741. [CrossRef]
5. Hatfield, J.L.; Dold, C. Water-use efficiency: Advances and challenges in a changing climate. *Front. Plant Sci.* **2019**, *10*, 103. [CrossRef]
6. Jensen, M.E. Water consumption by agricultural plants. In *Water Deficits and Plant Growth*; Kozlowski, T.T., Ed.; Academic Press: New York, NY, USA, 1968; Volume 2, pp. 1–22.
7. Allen, R.G.; Pereira, L.S.; Raes, D.; Smith, M. *Crop Evapotranspiration—Guidelines for Computing Crop Water Requirements*; FAO Irrigation and drainage paper 56; FAO: Rome, Italy, 1998; Volume 300, p. DO51909.
8. Howell, T.A.; Schneider, A.D.; Dusek, D.A.; Marek, T.H.; Steiner, J.L. Calibration and scale performance of Bushland weighing lysimeters. *Trans. ASAE* **1995**, *38*, 1019–1024. [CrossRef]
9. Baldocchi, D.; Falge, E.; Gu, L.; Olson, R.; Hollinger, D.; Running, S.; Anthoni, P.; Bernhofer, C.; Davis, K.; Evans, R.; et al. FLUXNET: A new tool to study the temporal and spatial variability of ecosystem- scale carbon dioxide, water vapor and energy flux densities. *Bull. Am. Meteorol. Soc.* **2001**, *82*, 2415–2434. [CrossRef]
10. Irmak, S.; Payero, J.O.; Kilic, A.; Odhiambo, L.; Sharma, V.; Rudnick, D.; Billesbach, D. On the magnitude and dynamics of eddy covariance residual energy (energy closure) from a subsurface drip-irrigated maize field during growing and non-growing (dormant) seasons. *Irrig. Sci.* **2014**, *32*, 471–483. [CrossRef]
11. Bowen, I.S. The ratio of heat losses by conduction and by evaporation from any water surface. *Phys. Rev.* **1626**, *27*, 779. [CrossRef]
12. Irmak, S.; Odhiambo, L.; Specht, J.E.; Djaman, K. Hourly and daily single and basal evapotranspiration crop coefficients as a function of growing degree days, days after emergence, leaf area index, fractional green canopy cover, and plant phenology for soybean. *Trans. ASABE* **2013**, *56*, 1785–1803.
13. Irmak, S.; Kukal, M.S. Alteration in surface energy balance fluxes induced from long-term disk- tilled versus no-till management in maize production. *Soil Tillage Res.* **2022**, *221*, 105383. [CrossRef]
14. Vertessy, R.; Hatton, T.; Reece, P.; O'sullivan, S.; Benyon, R. Estimating stand water use of large mountain ash trees and validation of the sap flow measurement technique. *Tree Physiol.* **1997**, *17*, 747–756. [CrossRef]
15. Hemakumara, H.M.; Chandrapala, L.; Moene, A.F. Evapotranspiration fluxes over mixed vegetation areas measured from large aperture scintillometer. *Agric. Water Manag.* **2003**, *58*, 109–122. [CrossRef]
16. Kohsiek, W.; Meijninger, W.M.L.; Moene, A.F.; Heusinkveld, B.G.; Hartogensis, O.K.; Hillen, W.C.A.M.; De Bruin, H.A.R. An Extra Large Aperture Scintillometer For Long Range Applications. *Bound.-Lay. Meteorol.* **2002**, *105*, 119–127. [CrossRef]
17. Meijninger, W.M.L.; Hartogensis, O.K.; Kohsiek, W.; Hoedjes, J.C.B.; Zuurbier, R.M.; De Bruin, H.A.R. Determination of Area-Averaged Sensible Heat Fluxes with a Large Aperture Scintillometer over a Heterogeneous Surface—Flevoland Field Experiment. *Bound.-Lay. Meteorol.* **2002**, *105*, 37–62. [CrossRef]
18. Bastiaanssen, W.G.; Menenti, M.; Feddes, R.A.; Holtslag, A.A.M. A Remote Sensing Surface Energy Balance Algorithm for Land (SEBAL). 1. Formulation. *J. Hydrol.* **1998**, *212*, 198–212. [CrossRef]
19. De Troch, F.P.; Troch, P.A.; Su, Z.; Lin, D.S. Application of Remote Sensing for Hydrological Modelling. In *Distributed Hydrological Modelling*; Springer: Dordrecht, The Netherlands, 1990; pp. 165–191.
20. Kustas, W.; Anderson, M. Advances in Thermal Infrared Remote Sensing for Land Surface Modeling. *Agric. For. Meteorol.* **2009**, *149*, 2071–2081. [CrossRef]
21. Liou, Y.A.; Kar, S.K. Evapotranspiration Estimation with Remote Sensing and Various Surface Energy Balance Algorithms—A Review. *Energies* **2014**, *7*, 2821–2849. [CrossRef]
22. García-Santos, V.; Sánchez, J.M.; Cuxart, J. Evapotranspiration Acquired with Remote Sensing Thermal-Based Algorithms: A State-of-the-Art Review. *Remote Sens.* **2022**, *14*, 3440. [CrossRef]
23. Allen, R.G.; Irmak, A.; Trezza, R.; Hendrickx, J.M.H.; Bastiaanssen, W.; Kjaersgaard, J. Satellite-based ET estimation in agriculture using SEBAL and METRIC. *Hydrol. Process* **2011**, *25*, 4011–4027. [CrossRef]
24. Fisher, J.B.; Melton, F.; Middleton, E.; Hain, C.; Anderson, M.; Allen, R.; McCabe, M.F.; Hook, S.; Baldocchi, D.; Townsend, P.A. The Future of Evapotranspiration: Global Requirements for Ecosystem Functioning, Carbon and Climate Feedbacks, Agricultural Management, and Water Resources. *Water Resour. Res.* **2017**, *53*, 2618–2626. [CrossRef]
25. Anderson, M.; Yang, Y.; Xue, J.; Knipper, K.; Yang, Y.; Gao, F.; Hain, C.; Kustas, W.P.; Cawse-Nicholson, K.; Hulley, G.; et al. Interoperability of ECOSTRESS and Landsat for Mapping Evapotranpiration Time Series at Sub-Field Scale. *Remote Sens. Environ.* **2021**, *252*, 112189. [CrossRef]
26. Senay, G.B.; Friedrichs, M.; Morton, C.; Parrish, G.E.L.; Schauer, M.; Khand, K.; Kagone, S.; Boiko, O.; Huntington, J. Mapping actual evapotranspiration using Landsat for the conterminous United States: Google Earth Engine implementation and assessment of the SSEBop model. *Remote Sens. Environ.* **2022**, *275*, 113011. [CrossRef]
27. Menenti, M.; Azzali, S.; Verhoef, W.; van Swol, R. Mapping agroecological zones and time lag in vegetation growth by means of Fourier analysis of time series of NDVI images. *Adv. Space Res.* **1993**, *13*, 233–237. [CrossRef]
28. Roerink, G.J.; Su, Z.; Menenti, M. S-SEBI: A Simple Remote Sensing Algorithm to Estimate the Surface Energy Balance. *Phys. Chem. Earth—Part B Hydrol. Ocean. Atmos.* **2000**, *25*, 147–157. [CrossRef]

29. Su, Z.; Abreham, Y.; Jun, W.; Roerink, G.; He, Y.; Gao, B.; Boogaard, H.; van Diepen, C. Assessing relative soil moisture with remote sensing data: Theory, experimental validation, and application to drought monitoring over the North China Plain. *Phys. Chem. Earth Parts A/B/C* **2003**, *28*, 89–101. [CrossRef]
30. Melton, F.S.; Johnson, L.F.; Lund, C.P.; Pierce, L.L.; Michaelis, A.R.; Hiatt, S.H.; Guzman, A.; Adhikari, D.D.; Purdy, A.J.; Rosevelt, C.; et al. Satellite Irrigation Management Support With the Terrestrial Observation and Prediction System: A Framework for Integration of Satellite and Surface Observations to Support Improvements in Agricultural Water Resource Management. *IEEE J. Sel. Top. Appl. Earth Obs. Remote. Sens.* **2012**, *5*, 1709–1721. [CrossRef]
31. Melton, F.S.; Huntington, J.; Grimm, R.; Herring, J.; Hall, M.; Rollison, D.; Erickson, T.; Allen, R.; Anderson, M.; Fisher, J.B.; et al. OpenET: Filling a critical data gap in water management for the Western United States. *J. Am. Water Resour. Assoc.* **2021**, *58*, 971–994. [CrossRef]
32. Volk, J.M.; Huntington, J.; Melton, F.S.; Allen, R.; Anderson, M.C.; Fisher, J.B.; Kilic, A.; Senay, G.; Halverson, G.; Knipper, K.; et al. Development of a Benchmark Eddy Flux Evapotranspiration Dataset for Evaluation of Satellite-Driven Evapotranspiration Models Over the CONUS. *Agric. For. Meteorol.* **2023**, *331*, 109307. [CrossRef]
33. Nassar, A.; Tarboton, D.G.; Gochis, D.; Melton, F.S. Evaluating the National Water Model's Evapotranspiration Representation through Comparison to OpenET. In *AGU Fall Meeting Abstracts*; AGU: Washington, DC, USA, 2022; p. H55E-03.
34. Cozzetto, K.; Chief, K.; Dittmer, K.; Brubaker, M.; Gough, R.; Souza, K.; Ettawageshik, F.; Wotkyns, S.; Opitz-Stapleton, S.; Duren, S.; et al. Climate change impacts on the water resources of American Indians and Alaska Natives in the U.S. *Clim. Chang.* **2013**, *120*, 569–584. [CrossRef]
35. Prein, A.; Holland, G.J.; Rasmussen, R.M.; Clark, M.P.; Tye, M.R. Running dry: The U.S. Southwest's drift into a drier climate state. *Geophys. Res. Lett.* **2016**, *43*, 1272–1279. [CrossRef]
36. Smith, A.B.; Katz, R.W. US billion-dollar weather and climate disasters: Data sources, trends, accuracy, and biases. *Nat. Hazards* **2013**, *67*, 387–410. [CrossRef]
37. Cayan, D.R.; Das, T.; Pierce, D.W.; Barnett, T.P.; Tyree, M.; Gershunov, A. Future dryness in the southwest US and the hydrology of the early 21st-century drought. *Proc. Natl. Acad. Sci. USA* **2010**, *107*, 21271–21276. [CrossRef] [PubMed]
38. Mohammed, A.T.; Irmak, S.; Kranz, W.L.; van Donk, S.; Yonts, C.D. Grain yield, crop and base evapotranspiration, production functions and water productivity response of drought-tolerant and non-drought tolerant maize hybrids under different irrigation levels, population densities: Part I. In western Nebraska's semi-arid environments. *Appl. Eng. Agric.* **2019**, *35*, 61–81.
39. Irmak, S.; Mohammed, A.T.; Kranz, W.L. Grain yield, crop and base evapotranspiration, production functions and water productivity response of drought-tolerant and non-drought tolerant maize hybrids under different irrigation levels, population densities and environments: Part II. In South-central and northeast Nebraska's transition zone and sub-humid environments. *Appl. Eng. Agric.* **2019**, *35*, 83–102.
40. Arnold, J.G.; Srinivasan, R.; Muttiah, R.S.; Allen, P.M. Continental Scale Simulation of the Hydrologic Balance. *J. Am. Water Resour. Assoc.* **1999**, *35*, 1037–1051. [CrossRef]
41. Djaman, K.; Koudahe, K.; Bodian, A.; Diop, L.; Ndiaye, P.M. Long-Term Trend Analysis in Annual and Seasonal Precipitation, Maximum and Minimum Temperatures in the Southwest United States. *Climate* **2020**, *8*, 142. [CrossRef]
42. Djaman, K.; O'Neill, M.; Owen, C.K.; Smeal, D.; Koudahe, K.; West, M.; Allen, S.; Lombard, K.; Irmak, S. Crop evapotranspiration, irrigation water requirement and water productivity of maize from meteorological data under semiarid climate. *Water* **2018**, *10*, 405. [CrossRef]
43. Barnes, F. Estimating Crop Water Requirement in Arizona and New Mexico. Master's Thesis, Department of Hydrology and Water Resources, The University of Arizona, Tucson, AZ, USA, 2011.
44. Djaman, K.; Allen, S.; Djaman, D.S.; Koudahe, K.; Irmak, S.; Puppala, N.; Darapuneni, M.K.; Angadi, S.V. Planting date and plant density effects on maize growth, yield and water use efficiency. *Environ. Chall.* **2022**, *6*, 100417. [CrossRef]
45. Sammis, T.W.; Mapel, C.L.; Lugg, D.G.; Lansford, R.R.; McGuckin, J.T. Evapotranspiration crop coefficients predicted using growing-degree days. *Trans. ASAE* **1985**, *28*, 773–780. [CrossRef]
46. Anderson, M.C.; Norman, J.M.; Mecikalski, J.R.; Otkin, J.A.; Kustas, W.P. A Climatological Study of Evapotranspiration and Moisture Stress across the Continental United States Based on Thermal Remote Sensing: 1. *Model Formulation, Journal of Geophysical Research: Atmospheres* **2007**, *112*, D10117.
47. Anderson, M.; Gao, F.; Knipper, K.; Hain, C.; Dulaney, W.; Baldocchi, D.; Eichelmann, E.; Hemes, K.; Yang, Y.; Medellin-Azuara, J.; et al. Field-Scale Assessment of Land and Water Use Change over the California Delta Using Remote Sensing. *Remote Sens.* **2018**, *10*, 889. [CrossRef]
48. Allen, R.G.; Tasumi, M.; Morse, A.; Trezza, R. A Landsat-Based Energy Balance and Evapotranspiration Model in Western US Water Rights Regulation and Planning. *Irrig. Drain. Syst.* **2005**, *19*, 251–268. [CrossRef]
49. Allen, R.G.; Tasumi, M.; Trezza, R. Satellite-Based Energy Balance for Mapping Evapotranspiration with Internalized Calibration (METRIC) Model. *J. Irrig. Drain. Eng.* **2007**, *133*, 380–394. [CrossRef]
50. Allen, R.G.; Pereira, L.S.; Howell, T.A.; Jensen, M.E. Evapotranspiration Information Reporting: I. Factors Governing Measurement Accuracy. *Agric. Water Manag.* **2011**, *98*, 899–920. [CrossRef]
51. Laipelt, L.; Kayser, R.H.B.; Fleischmann, A.S.; Ruhoff, A.; Bastiaanssen, W.; Erickson, T.A.; Melton, F. Long-Term Monitoring of Evapotranspiration Using the SEBAL Algorithm and Google Earth Engine Cloud Computing. *ISPRS J. Photogramm. Remote Sens.* **2021**, *178*, 81–96. [CrossRef]

52. Fisher, J.B.; Tu, K.P.; Baldocchi, D.D. Global Estimates of the Land–Atmosphere Water Flux Based on Monthly AVHRR and ISLSCP-II Data, Validated at 16 FLUXNET Sites. *Remote Sens. Environ.* **2008**, *112*, 901–919. [CrossRef]
53. Pereira, L.S.; Paredes, P.; Melton, F.; Johnson, L.; Wang, T.; López-Urrea, R.; Cancela, J.J.; Allen, R.G. Prediction of crop coefficients from fraction of ground cover and height background and validation using ground and remote sensing data. *Agric. Water Manag.* **2020**, *241*, 106197. [CrossRef]
54. Senay, G.B.; Bohms, S.; Singh, R.K.; Gowda, P.H.; Velpuri, N.M.; Alemu, H.; Verdin, J.P. Operational Evapotranspiration Mapping Using Remote Sensing and Weather Datasets: A New Parameterization for the SSEB Approach. *J. Am. Water Res. Assoc.* **2013**, *49*, 577–591. [CrossRef]
55. Senay, G.B. Satellite Psychrometric Formulation of the Operational Simplified Surface Energy Balance (SSEBop) Modelfor Quantifying and Mapping Evapotranspiration. *Appl. Eng. Agric.* **2018**, *34*, 555–566. [CrossRef]
56. Cammalleri, C.; Anderson, M.C.; Gao, F.; Hain, C.R.; Kustas, W.P. A Data Fusion Approach for Mapping Daily Evapotranspiration at Field Scale. *Water Resour. Res.* **2013**, *49*, 4672–4686. [CrossRef]
57. Cardinali, A.; Nason, G.P. Costationarity of Locally Stationary Time Series Using costat. *J. Stat. Softw.* **2013**, *55*, 1–22. [CrossRef]
58. Senay, G.B.; Schauer, M.; Friedrichs, M.; Velpuri, N.M.; Singh, R.K. Satellite-based water use dynamics using historical Landsat data (1984–2014) in the southwestern United States. *Remote Sens. Environ.* **2017**, *202*, 98–112. [CrossRef]
59. Senay, G.B.; Schauer, M.; Velpuri, N.M.; Singh, R.K.; Kagone, S.; Friedrichs, M.; Litvak, M.E.; Douglas-Mankin, K.R. Long-term (1986–2015) crop water use characterization over the upper Rio Grande Basin of United States and Mexico using landsat-based evapotranspiration. *Remote Sens.* **2019**, *11*, 1587. [CrossRef]
60. de Oliveira, M.L.; dos Santos, C.A.C.; Santos, F.A.C.; de Oliveira, G.; Santos, C.A.G.; Bezerra, U.A.; de BL Cunha, J.E.; da Silva, R.M. Evaluation of Water and Carbon Estimation Models in the Caatinga Biome Based on Remote Sensing. *Forests* **2023**, *14*, 828. [CrossRef]
61. Kayser, R.H.; Ruhoff, A.; Laipelt, L.; de Mello Kich, E.; Roberti, D.R.; de Arruda Souza, V.; Cristina Dotto Rubert, G.; Collischonn, W.; Neale, C.M.U. Assessing geeSEBAL automated calibration and meteorological reanalysis uncertainties to estimate evapotranspiration in subtropical humid climates. *Agric. Forest Meteo.* **2022**, *314*, 108775. [CrossRef]
62. Gonçalves, I.Z.; Ruhoff, A.; Laipelt, L.; Bispo, R.C.; Hernandez, F.B.T.; Neale, C.M.U.; Teixeira, A.H.C.; Marin, F.R. Remote sensing-based evapotranspiration modeling using geeSEBAL for sugarcane irrigation management in Brazil. *Agric. Water Manag.* **2022**, *274*, 107965. [CrossRef]
63. Wei, G.; Cao, J.; Xie, H.; Xie, H.; Yang, Y.; Wu, C.; Cui, Y.; Luo, Y. Spatial-Temporal Variation in Paddy Evapotranspiration in Subtropical Climate Regions Based on the SEBAL Model: A Case Study of the Ganfu Plain Irrigation System, Southern China. *Remote Sens.* **2022**, *14*, 1201. [CrossRef]
64. Kilic, A.; Allen, R.G.; Blankenau, P.; Revelle, P.; Ozturk, D.; Huntington, J. Global production and free access to Landsat-scale Evapotranspiration with EEFlux and eeMETRIC. In Proceedings of the 6th Decennial National Irrigation Symposium, American Society of Agricultural and Biological Engineers, San Diego, CA, USA, 6–8 December 2021; pp. 2020–2038.
65. Ortega-Salazar, S.; Ortega-Farías, S.; Kilic, A.; Allen, R. Performance of the METRIC model for mapping energy balance components and actual evapotranspiration over a superintensive drip-irrigated olive orchard. *Agric. Water Manag.* **2021**, *251*, 106861. [CrossRef]
66. Jaafar, H.H.; Mourad, R.M.; Kustas, W.P.; Anderson, M.C. A global implementation of single- and dual-source surface energy balance models for estimating actual evapotranspiration at 30-m resolution using Google Earth Engine. *Water Resour. Res.* **2022**, *58*, e2022WR032800. [CrossRef]
67. Komatsu, T.S. Toward a robust phenomenological expression of evaporation efficiency for unsaturated soil surfaces. *J. Appl. Meteorol.* **2003**, *42*, 1330–1334. [CrossRef]
68. Agam, N.; Kustas, W.P.; Anderson, M.C.; Norman, J.M.; Colaizzi, P.D.; Howell, T.A.; Prueger, J.H.; Meyers, T.P.; Wilson, T.B. Application of the Priestley–Taylor approach in a two-source surface energy balance model. *J. Hydrometeorol.* **2010**, *11*, 185–198. [CrossRef]
69. Talsma, C.J.; Good, S.P.; Jimenez, C.; Martens, B.; Fisher, J.B.; Miralles, D.G.; McCabe, M.F.; Purdy, A.J. Partitioning of evapotranspiration in remote sensing-based models. *Agric. For. Meteorol.* **2018**, *260–261*, 131–143. [CrossRef]
70. Luo, Z.; Guo, M.; Bai, P.; Li, J. Different Vegetation Information Inputs Significantly Affect the Evapotranspiration Simulations of the PT-JPL Model. *Remote Sens.* **2022**, *14*, 2573. [CrossRef]
71. Doherty, C.T.; Johnson, L.F.; Volk, J.; Mauter, M.S.; Bambach, N.; McElrone, A.J.; Alfieri, J.G.; Hipps, L.E.; Prueger, J.H.; Castro, S.J.; et al. Effects of meteorological and land surface modeling uncertainty on errors in winegrape ET calculated with SIMS. *Irrig. Sci.* **2022**, *40*, 515–530. [CrossRef] [PubMed]
72. Srivastava, A.; Sahoo, B.; Raghuwanshi, N.S.; Singh, R. Evaluation of Variable-Infiltration Capacity Model and MODIS-Terra Satellite-Derived Grid-Scale Evapotranspiration Estimates in a River Basin with Tropical Monsoon-Type Climatology. *J. Irrig. Drain. Eng.* **2017**, *143*, 04017028. [CrossRef]
73. Basso, B.; Ritchie, J.T. Evapotranspiration in High-Yielding Maize and under Increased Vapor Pressure Deficit in the US Midwest. *Agric. Environ. Lett.* **2018**, *3*, 170039. [CrossRef]
74. Djaman, K.; Irmak, S.; Rathje, W.R.; Martin, D.L.; Eisenhauer, D.E. Maize evapotranspiration, yield production function, biomass, grain yield, harvest index, and yield response factors under full and limited irrigation. *Trans. ASABE* **2013**, *56*, 273–293.
75. Trout, T.J.; DeJonge, K.C. Water productivity of maize in the US high plains. *Irrig. Sci.* **2017**, *35*, 251–266. [CrossRef]

76. Pablo, R.G.; O'Neill, M.K.; McCaslin, B.D.; Remmenga, M.D.; Keenan, J.G.; Onken, B.M. Evaluation of Corn Grain Yield and Water Use Efficiency Using Subsurface Drip Irrigation. *J. Sustain. Agric.* **2007**, *30*, 153–172. [CrossRef]
77. Hao, B.; Xue, Q.; Marek, T.H.; Jessup, K.E.; Becker, J.; Hou, X.; Xu, W.; Bynum, E.D.; Bean, B.W.; Colaizzi, P.D.; et al. Water use and grain yield in drought-tolerant corn in the Texas High Plains. *Agron. J.* **2015**, *107*, 1922–1930. [CrossRef]
78. Colaizzi, P.D.; Evett, S.R.; Howell, T.A. Corn production with spray, LEPA, and SDI. In Proceedings of the 23rd Annual Central Plains Irrigation Conference, Burlington, CO, USA, 22–23 February 2011; Central Plains Irrigation Association: Colby, KS, USA, 2011; pp. 52–67.
79. Yazar, A.; Howell, A.T.; Dusek, D.A.; Copeland, K.S. Evaluation of crop water stress index for LEPA irrigated corn. *Irrig. Sci.* **1999**, *18*, 171–180. [CrossRef]
80. Schneider, A.D.; Howell, T.A. LEPA and spray irrigation of corn-Southern High Plains. *Trans. Am. Soc. Agric. Eng.* **1998**, *41*, 1391–1396. [CrossRef]